

Modeling of Cu Direct Laser Drilling Process

Junichi OKADA^{*1}, Yuuji OKAMOTO^{*1}, Kazumasa SHUDO^{*1} and Masafumi YOROZU^{*1}

^{*1} Sumitomo Heavy Industries, Ltd. Mechanical System Engineering Dept. Research & Development Center, 19, Natsushima-cho, Yokosuka-shi, Kanagawa 237-8555, Japan
E-mail: Jnc_Okada@shi.co.jp

Drilling of printed wiring boards (PWBs) by CO₂ laser radiation was studied both experimentally and theoretically. Two types of processes are generally used for drilling: resin direct drilling (RDD) and Cu direct drilling (CDD). RDD is a single-layer removal process and is explained using the evaporative removal model under the condition that the laser pulse width exceeds a nanosecond. In this model, the processed material evaporates upon heating by a laser beam. In the CDD process, Cu and resin layers are simultaneously removed. However, Cu and resin have different physical characteristics. Therefore, the evaporative removal model cannot be applied to the CDD process, and a new model is required. An experimental study of CDD shows that via holes open at a certain irradiation energy. Thermal simulation revealed that the thermal decomposition of the resin interface is complete before copper is evaporated. These results show that as a result of thermal decomposition, resin's internal pressure increases rapidly and the pressure pushes upward the liquid Cu foil in the upper layer. Then, the vaporized resin scatters liquid copper. Furthermore, the via hole shape can be calculated using this model.

DOI: 10.2961/jlmn.2012.03.0024

Keywords: Laser drilling, Printed wiring board, CO₂ laser, Heat transfer analysis, Cu direct drilling

1. Introduction

With the rapid spread and high performance of portable digital devices such as mobile phones, the use of multistratified printed wiring boards (PWBs) has become widespread. In a multistratified PWB, a via hole is processed to connect the upper layer with the lower layer by using wired connections. To drill this hole, high-speed processing is required. Therefore, laser drilling is widely used for via hole processing.

Two types of laser sources are used to drill PWBs: CO₂ lasers (emission wavelength in the infrared region) and UV lasers. The CO₂ laser process can drill faster than the UV laser process. For the reason that the CO₂ laser is able to oscillate significant power, the CO₂ laser process needs fewer pulse number than the UV laser process.

Fig. 1 shows the typical approach to CO₂ laser drilling. In the preprocessing step, a window is formed in the outer Cu layer of a PWB by conformal and large window drilling processes to enable direct irradiation of the resin layer with the CO₂ laser. The resin layer is composed of woven fiberglass cloth with an epoxy resin. To optimize the size, we consider the resin direct drilling (RDD) process, which follows a single-layer removal model.

In contrast, in Cu direct drilling (CDD), the outer Cu and resin layers are simultaneously removed, and a via hole is formed. This process is considered to follow the multi-layer structure removal model.

In previous studies ^{[1], [2]}, the RDD model (including conformal and large window processes) was established. Furthermore, improvements in the shape of the via hole in the resin layer have been studied ^[3]. CDD has also been studied experimentally. However, there is no clear understanding of a detailed model of the process involved.

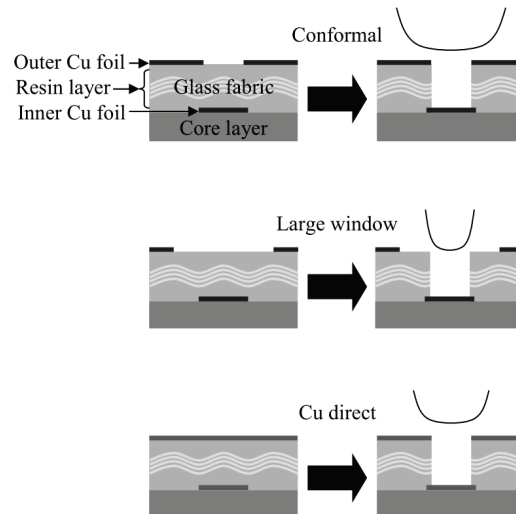


Fig. 1 Via hole drilling process

Therefore, this paper describes the mechanism of via hole formation by CDD.

1.1 Resin direct drilling (RDD)

The resin layer acts as an insulation layer between the outer and inner Cu layers and it primarily consists of an epoxy resin. To improve the strength of PWBs, FR-4 prepreg impregnated woven glass fabric is often used.

In conformal drilling, the open window diameter is usually equal to the via hole diameter, and the outer Cu foil acts as a masking material.

The large window drilling method uses a beam diameter that is almost 50-100 μm smaller than the window diameter.

1.2 Cu direct drilling (CDD)

In CDD, the outer Cu layer is directly irradiated by a CO₂ laser in the infrared range. However, infrared absorptance of an untreated Cu surface is very low (approximately 5%). To solve this problem, surface treatment of the outer Cu layer is required. Possible treatments include black oxidation and various roughening processes. Surface treatment changes the outer Cu surface typically 12 µm thick into an oxidized film approximately 2 µm thick. This increases the surface infrared absorptance from 5% to 20%–70%.

2. Experimental method

2.1 Optical setup

Fig. 2 shows the optical setup of a CO₂ laser drilling machine that has a control system for the spatial and temporal beam profiles.

The laser light source is a CO₂ laser with a wavelength of 9.3µm, laser pulse width is 2-800us, and average power is more than 280W. The spatial beam profile at the working surface can be controlled by the use of various optical systems. Variable beam shaper in Fig.2 has a telecentric optical system with aspheric lens. This optical setup results in optical transcription from the mask surface to the working surface.

Fig. 3 shows the spatial beam profile of each surface. The temporal beam profile is a square wave, and the pulse width is controllable.

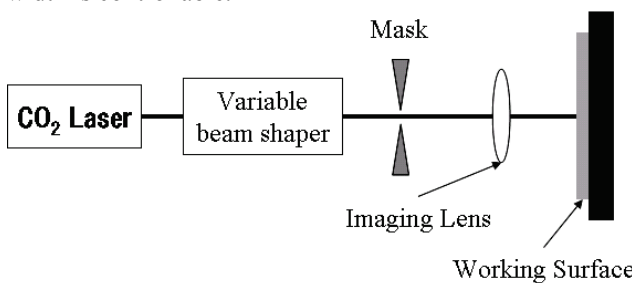


Fig. 2 Optical setup of CO₂ laser drilling machine involving laser source, mask surface, and working surface

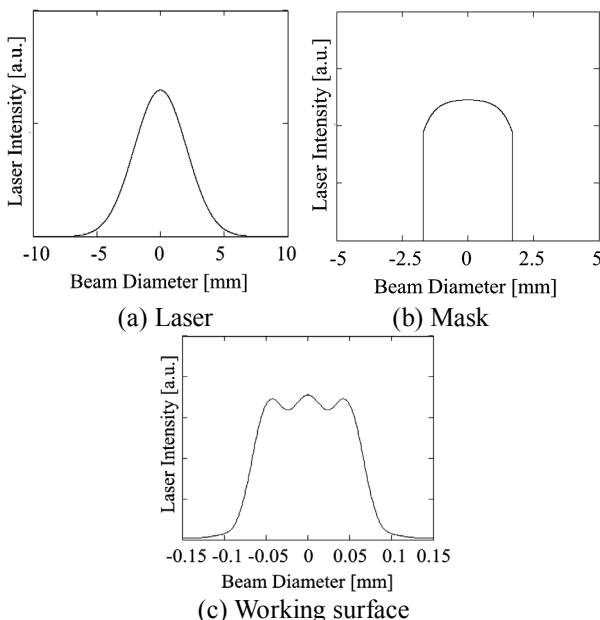


Fig. 3 Spatial beam profile control

2.2 Experimentally determined relationship between irradiation energy and hole shape

The drilling properties of RDD and CDD were compared. Table 1 lists the experimental conditions. The irradiation energy can be controlled by varying the pulse width. The material used in RDD does not have an outer Cu layer, whereas the CDD material is covered by a black oxide film (thickness: 2 µm, surface infrared absorptance: 25%).

Fig. 4 shows the relationship between irradiation energy and hole diameter. The hole diameter in case of RDD processing increases with the irradiation energy. However, in case of CDD processing, a certain energy threshold range (4.2–6.6 mJ) must be reached to penetrate the outer Cu layer. If the irradiation energy is larger than 6.6 mJ, the hole diameter is unchanged.

Table 1 Experimental conditions

Material conditions		
Type	Resin direct	Cu direct
Cu thickness		12µm
Resin thickness	55 µm	60µm
Laser conditions		
Beam diameter	160µm	160µm
Spatial beam profile	Flat top	Flat top
Temporal beam profile	Square	Square
Irradiation energy	1.1-8.7 mJ	1.0-11.5 mJ

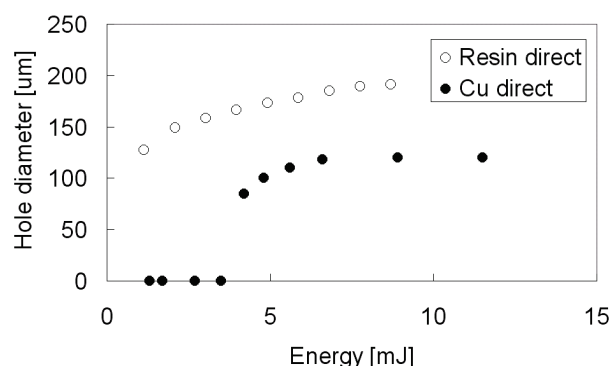


Fig. 4 Relationship between irradiation energy and hole diameter

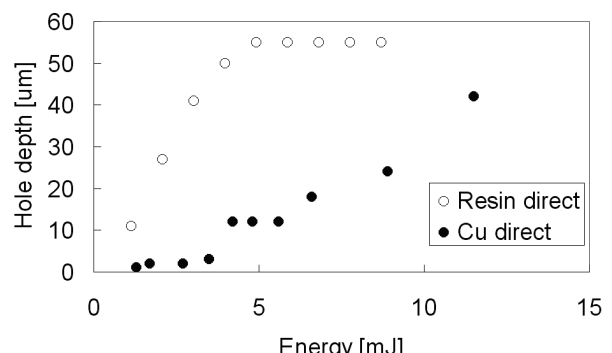


Fig. 5 Relationship between irradiation energy and hole depth

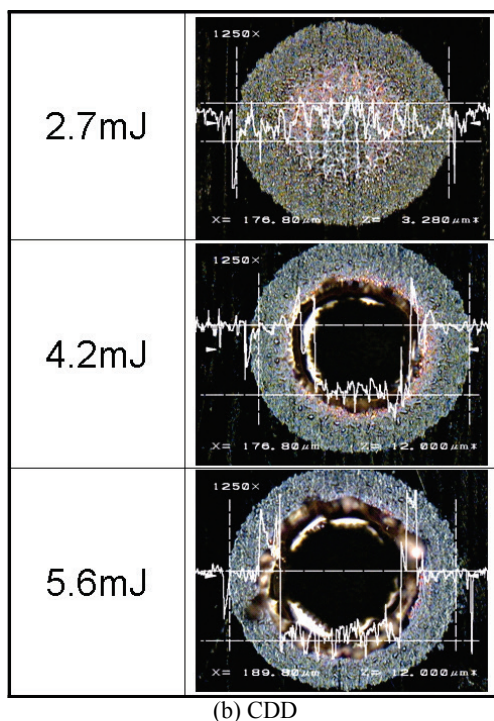
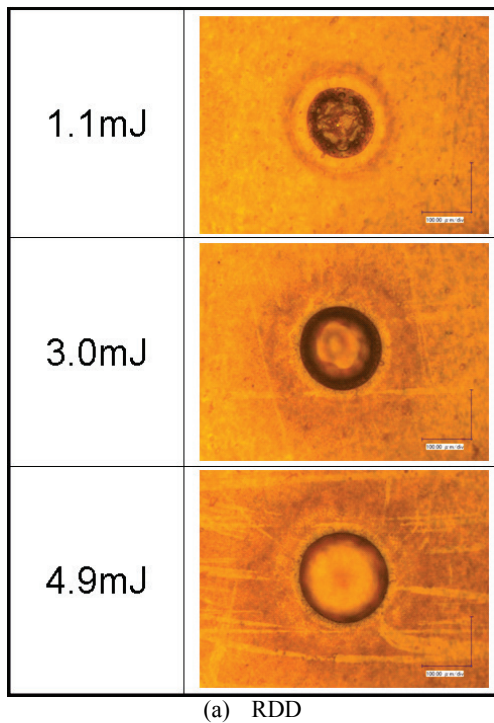


Fig. 6 Top views of via hole

Fig.5 shows the relationship between irradiation energy and hole depth. The graph of the hole depth in CDD exhibits a plateau at an energy of 4.2–5.6 mJ and a hole depth of 12 μm . This indicates that drilling of the resin layer is not observed when the energy is sufficiently high to pass through the outer Cu layer.

Fig.6 shows top views of the via holes. In CDD, the scattered Cu foil does not appear to be vaporized.

3. Process simulation

3.1 Flow chart

The purpose of this process simulation is to determine the shape of the via hole. Fig. 7 shows a flow chart of the method. The simulation is divided into the following two calculation stages:

- 1) Simulation of light propagation considering diffraction
- 2) Solving the heat equation to determine the state of each layer

The method of optical simulation with light propagation considering diffraction is explained in [4]. The simulation results are shown in Fig. 3(c).

We measure the experimental spatial beam profile of the working surface by using the shape of the laser-drilled hole of a polyimide film. Polyimide film exhibits a spatial beam profile. This result agrees with the experimental spatial beam profile of the working surface.

In Section 3.3, we explain the method of solving the heat equation (2D unsteady conduction analysis with the finite difference method, FDM) to determine the state of each layer.

After the decision state (solid/liquid/vapor/pyrolysis gas), this simulation determines whether ablation was complete for each mesh and it generally uses the evaporative removal model [5]. For this model to be applicable, the laser pulse width must exceed 1 ns, and the laser emission wavelength must be in the visible to infrared range. Therefore, the CO₂ laser drilling process was considered to follow this model.

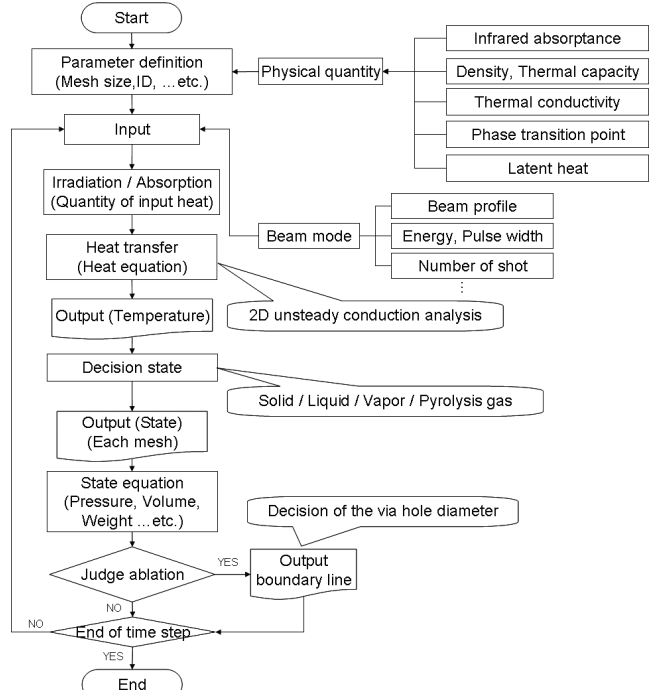


Fig. 7 Flow chart of drilling process simulation

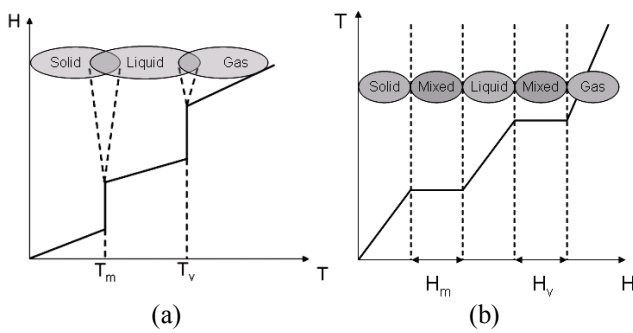


Fig. 8 State diagram

3.2 Input parameters

Actual measurement values were used for the thermal properties of each PWB material. Typical physical characteristics of the materials are shown in Table 2.

Note that the absorptance of the treated Cu surface (CuO) differs for each PWB. To correctly measure absorptance, we selected an infrared thermography technique reported in an earlier study [6].

The decomposition heat of each epoxy resin also differs for each PCB. We selected a technique that uses thermogravimetric analysis-differential scanning calorimetry (TGA-DSC). TGA determines changes in the weight of a sample relative to temperature. DSC is a thermoanalytical technique in which the difference in the amount of heat required to increase the temperature of a sample and that of a reference is measured as a function of temperature.

Total heat absorption obtained by TGA-DSC is then translated into the latent heat of decomposition.

3.3 Heat equation

The 2D heat transfer equation for an axisymmetric model is given by

$$\rho \cdot C_p \frac{\partial T}{\partial t} = \frac{1}{r} \frac{\partial}{\partial r} \left\{ \kappa \left(r \frac{\partial T}{\partial r} \right) \right\} + \frac{\partial}{\partial z} \left\{ \kappa \left(\frac{\partial T}{\partial z} \right) \right\} + Q \quad (1)$$

where, T is the temperature, ρ is the density, C_p is the thermal capacity, κ is the thermal conductivity, and Q is the quantity of the heat input. This quantity is considered as the source term, which is given by

$$Q = \alpha(1-R)I_0(t)F(r) \quad (2)$$

where, α is the absorption coefficient, R is the reflectance, I_0 is the time-dependent intensity of the pulse light, and $F(r)$ is the spatial beam profile of the working surface. This spatial beam profile is given by the simulation of light propagation considering diffraction, as shown in Fig.3(c).

When phase transitions occur, the effect of latent heat must be considered to solve the heat equation. The effect of latent heat is shown in the state diagram in Fig.8(a). At the melting point temperature, the material can be either solid, liquid, or a mixture of both.

We begin to reformulate the heat equation by defining the total change in enthalpy, as given in equation (3).

Table 2 Typical physical characteristics of the materials

Material	Cu	CuO	Epoxy resin
Density [g/cm ³]	8.95	6.76	1.72
Specific heat [J/gK]	0.39	0.53	0.95
Thermal conductivity [W/cm·K]	4.01	0.032	0.003
Infrared absorptance	0.05	0.2-0.7 (0.25)	0.8
Melting temp. [K] (Decomposition)	1357	1474	(370-1200)
Heat of melting [J/g] (Decomposition)	209	148	(807.9)
Absorption coefficient [1/cm]	7.7 × 10 ⁵	7.14 - 7.7 × 10 ⁵	1.0 × 10 ⁴
Evaporation temp. [K]	2840		

$$\Delta H(T) = \int_{T_0}^T \rho C_p dT + \xi(T - T_m) H_{latent,m} + \eta(T - T_v) H_{latent,v}$$

$$\xi(x) = \begin{cases} 1 & \text{when } x > 0 \\ 0 & \text{otherwise} \end{cases}$$

$$\eta(y) = \begin{cases} 1 & \text{when } y > 0 \\ 0 & \text{otherwise} \end{cases} \quad (3)$$

The integrand describes the heat input required to heat the solid to a temperature T , and the Heaviside function [$\xi(T - T_m)$] switches on the latent heat when the temperature exceeds the melting temperature (T_m). Partial differentiation of both sides of equation (3) gives

$$\frac{\partial H}{\partial t} = \rho C_p \frac{\partial T}{\partial t} \quad (4)$$

Substitution into equation (1) produces the enthalpy based heat equation below.

$$\frac{\partial H}{\partial t} = \frac{1}{r} \frac{\partial}{\partial r} \left\{ \kappa \left(r \frac{\partial T}{\partial r} \right) \right\} + \frac{\partial}{\partial z} \left\{ \kappa \left(\frac{\partial T}{\partial z} \right) \right\} + Q \quad (5)$$

This equation produces the state diagram shown in Fig.8(b), which is a one-to-one relationship between enthalpy and the separated state. Based on our simulation, equation (5) is translated into a difference formula.

3.4 Simulation results

The simulated relationships between irradiation energy and hole diameter are shown in Fig. 9. The experimental results (RDD: ○, CDD: ●) are shown for comparison with the simulation results (RDD: dashed line, CDD: solid line). The experimental and simulation results agree well in case of RDD. However, in case of CDD, a significant discrepancy is observed between these results. The experimental result for CDD shows that approximately 5 mJ of irradiation energy is needed to penetrate the Cu layer, whereas the simulation result for CDD shows that approximately 20 mJ of irradiation energy is necessary to evaporate the Cu layer. These results show that it is impossible to apply the evaporative removal model for CDD. Therefore, a new model is required.

3.5 Thermal analysis of CDD

To determine the decision state and time change of state, we performed thermal analysis of each CDD layer at the central beam axis. We analyzed the CDD material described in Table 1 with the following conditions: (1) thickness of materials: CuO: 2 μm , Cu: 10 μm , epoxy resin: 60 μm ; (2) laser conditions: irradiation energy: 11.5 mJ, irradiation time: 15 μs ; and (3) end of time step: 20 μs . The result is shown in Fig. 10.

Fig. 10 shows the phase transition temperature at the central beam axis of each layer calculated numerically by FDM. In Fig. 10, (\blacklozenge) denotes the temperature 0.25 μm below the top surface, (\triangle) denotes the temperature of the interface between CuO and Cu, (\bullet) denotes the temperature of the interface between Cu and the resin, and (\circ) denotes the temperature 0.25 μm below the Cu/resin interface. According to this result, the temperature of the surface layer, which consists of CuO, increases rapidly and the layer reaches the vapor phase. The top and bottom of the CuO layer are vaporized in approximately 1 and 10 μs , respectively. During this time, the heat is transferred from the CuO layer to the untreated Cu layer. The top and bottom Cu layers reach the melting point (1357K: solid line) after 7 and 12 μs , respectively. Although the Cu layer does not reach the vaporization point (2840 K), the resin layer under the liquid phase of Cu reaches the decomposition point (1200 K) after 12 μs owing to thermal conduction.

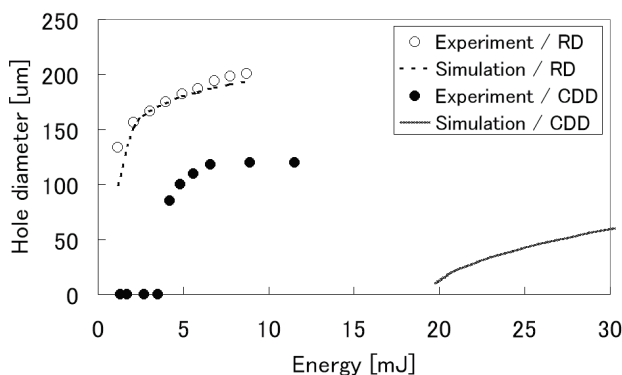


Fig. 9 Result of simulation using the evaporative removal model

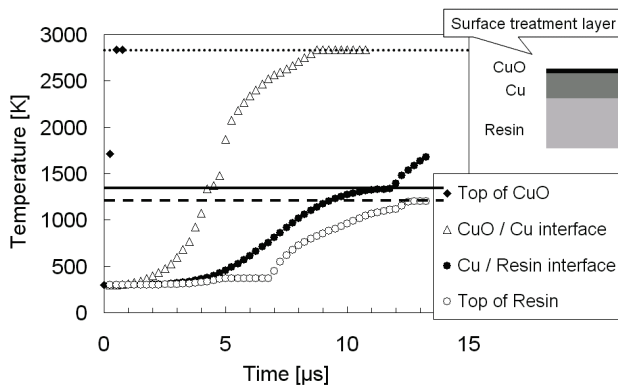


Fig. 10 Relationships between laser irradiation time and temperature for each layer

4. Discussion

4.1 Theoretical model

The experimental results for the CDD process show that the via hole opens at a certain irradiation energy, and the energy required to penetrate the outer Cu layer is approximately one-quarter of that necessary for evaporation of the Cu layer. Thermal analysis of the CDD process shows that thermal decomposition of the resin interface is complete before Cu is evaporated. These results suggest a new model, which is shown in Fig. 11. Owing to thermal conduction in the Cu layer, the rapid increase in the internal gas pressure of the resin can scatter liquid Cu and create a via hole. In this model, the area of liquid Cu area and the via hole are the same at the instant liquid Cu is scattered. Scattering releases the pressure between the resin and the Cu layers. Therefore, we can consider that the subsequent drilling process follows the evaporative removal model. The time of liquid Cu scattering is that at which the internal pressure of the resin is sufficient to increase the total weight of the liquid copper. We treat this model as the CDD model.

4.2 Simulation with CDD model

We adapted this CDD model to the process simulation of Fig. 7. The experimental and simulation results with this model are compared in Fig. 12.

Fig. 12(a) shows the relationship between irradiation energy and hole diameter. The simulation result is consistent with the experimentally measured data, and the threshold energy, which was significantly higher for the evaporative removal model, agrees with the experimentally measured one. However, there is still a difference of approximately 4 mJ between the model and experimental results. This is believed to be caused by the influence of glass fabric in the epoxy resin layer and scattering light at the interface between the CuO and Cu layers.

Fig. 12(b) shows the relationship between irradiation energy and hole depth. The experimental and simulation results both exhibit a plateau in the graph. If the required time for Cu scattering is longer than the pulse width, the laser beam cannot be used to directly drill the resin layer. Furthermore, experimental and simulation results of hole depth vary. It is thought that this difference is caused by the influence of the glass fabric in the epoxy resin layer because a significant difference is observed after liquid copper scattering.

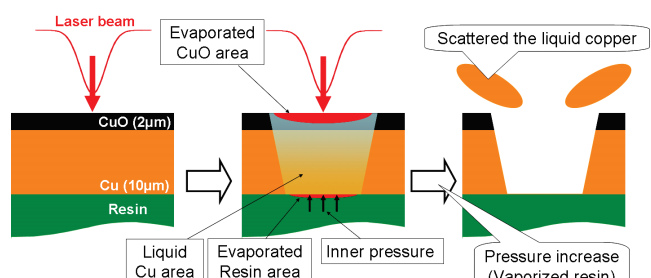
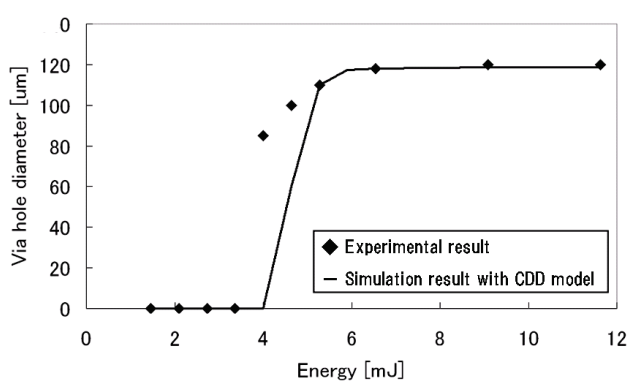
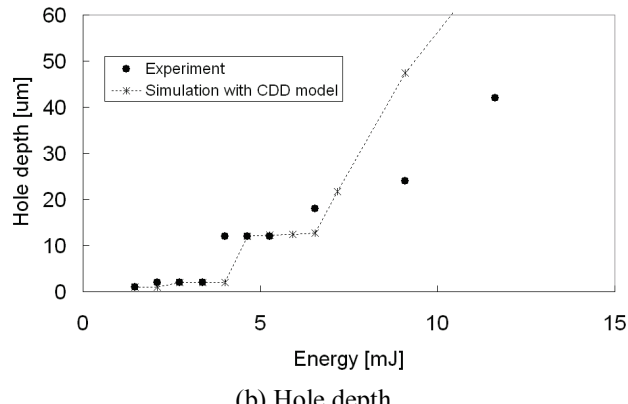


Fig. 11 Model of CDD



(a) Hole diameter



(b) Hole depth

Fig. 12 Simulation results with CDD model

5. Conclusion

By comparing the experimental and simulation results of the laser drilling process, we developed a CDD model with the following characteristics.

- 1) The single-layer removal process is described by the evaporative removal model.
- 2) In the model showing via hole formation with the CDD process, the area in which liquid Cu exists has the shape of the via hole before the liquid Cu foil is scattered.
- 3) The existence of a certain energy threshold is explained by the timing of liquid Cu scattering.

Using this new CDD model, we can present an approximate analysis of the via hole shape by using Cu direct laser drilling, and we can find the optimum laser irradiation condition. This model can also describe the laser drilled via hole shape of PCBs with treated and untreated Cu surfaces.

References

- [1] S. Noguchi, E. Ohmura, and I. Miyamoto: Journal of the Japan Society for Precision Engineering Papers, 69, (4), 536-541, (2003) in Japanese
- [2] T. Hirogaki, E. Aoyama, K. Ogawa, R. Minagi, T. Murakami and N. Doi: Journal of the Society of Materials Science Japan, 55, (3), 335-340, (2006) in Japanese
- [3] C. J. Moorhouse, F. Villarreal, J. J. Wendland, H. J. Baker, D.R. Hall and D.P. Hand: Proc. of SPIE, 276-283, (2004)
- [4] S. Noguchi and E. Ohmura: Journal of the Japan Society for Precision Engineering Papers, 71, (10), 1296-1302, (2005) in Japanese
- [5] D. Bauerle: "Laser Processing and chemistry" ed. by Springer-Verlag Berlin Heidelberg New York (Publisher, Germany, 1996) p.173. (Books)
- [6] T. Hirogaki, E. Aoyama, K. Ogawa, S. Matsutani and T. Ayuzawa: Transactions of the Japan Society of Mechanical Engineers. C 76(771), 3143-3149, (2011) in Japanese

(Received: June 10, 2011, Accepted: October 18, 2012)